ELSEVIER

Biochimica et Biophysica Acta 1570 (2002) 1–8

BIOCHIMICA ET BIOPHYSICA ACTA
BBA

www.bba-direct.com

Cell and nucleus deformation in compressed chondrocyte–alginate constructs: temporal changes and calculation of cell modulus

M.M. Knight [a,*], J. van de Breevaart Bravenboer [b], D.A. Lee [a], G.J.V.M. van Osch [b], H. Weinans [b], D.L. Bader [a]

[a] *Interdisciplinary Research Centre (IRC) in Biomedical Materials and Department of Engineering, Queen Mary University of London, Mile End Rd., London E1 4NS, UK*

[b] *Orthopaedic Research Laboratory, Erasmus University, Rotterdam, Netherlands*

Received 21 May 2001; received in revised form 6 December 2001; accepted 13 December 2001

Abstract

Mechanical loading is essential for the homeostasis of articular cartilage and may be necessary for achieving functional tissue engineered cartilage repair using isolated cells seeded in scaffolds such as alginate. Chondrocyte mechanotransduction is poorly understood, but may involve cell deformation and associated distortion of intracellular organelles. The present study used confocal microscopy to examine cell and nucleus morphology in isolated chondrocytes compressed in alginate constructs. Compression of 2% alginate resulted in cell deformation from a spherical to an oblate ellipsoid morphology with conservation of cell volume. Cell deformation was associated with deformation, to a lesser degree, of the nucleus. Despite constant cell deformation over a 25 min period of static compression, the nucleus deformation reduced significantly, particularly in the axis perpendicular to the applied compression. Constructs made of a lower alginate concentration exhibited a reduced compressive modulus with an altered cellular response to compression. In 1.2% alginate, compression resulted in cell deformation which was initially of a similar magnitude to that in 2% alginate but subsequently reduced over a 60 min period reflecting the viscoelastic behaviour of the gel. This phenomenon enabled the calculation of a stress–strain relationship for the cell with an estimated Young's modulus value of approx. 3 kPa.

Keywords: Chondrocyte; Mechanotransduction; Alginate; Deformation; Mechanics

1. Introduction

One tissue engineering strategy widely proposed for the repair of articular cartilage defects involves seeding isolated chondrocytes within biodegradable 3D scaffolds [1–3]. For this approach to be successful it may be necessary to stimulate the cells so that they rapidly elaborate a mechanically functional cartilaginous matrix. Recent studies have suggested that this may be achieved using mechanical loading, which is essential for the health and homeostasis of articular cartilage in vivo [4,5]. The process by which mechanical loading influences the metabolism of the chondrocytes and their synthesis of extracellular matrix is termed mechanotransduction. Physiological levels of stress applied to cartilage explants result in compression of the cartilage, by up to 20%, and associated deformation of the chondrocytes and their internal organelles [6–8]. The mechanotransduction pathways within cartilage remain unclear but may involve cell and nucleus deformation, hydrostatic pressure, electrical streaming potentials and changes in pH and osmotic pressure [9–11].

Mechanotransduction also occurs in isolated chondrocytes compressed in 3D scaffolds including agarose gel [5,12,13] and alginate gel [14]. Alginate, which is isolated from seaweed, is a negatively charged linear polysaccharide consisting of β-D-mannuronic acid and α-L-glucuronic acid [15]. In the presence of cations such as calcium, alginate polymerises to form a non-toxic hydrogel. Whilst agarose has been used primarily as a model system for

* Corresponding author. Fax: +44-20-89-83-17-99;
IRC web site: http://www.irc-biomed-materials.qmw.ac.uk/.
E-mail address: m.m.knight@qmul.ac.uk (M.M. Knight).

0304-4165/02/$ – see front matter
PII: S0304-4165(02)00144-7

investigating mechanotransduction in isolated cells, alginate gel is widely proposed as a suitable scaffold component for tissue engineered cartilage repair [16–19]. There is therefore increasing interest in the influence of mechanical loading on isolated chondrocytes in alginate scaffolds. In order to understand and optimise any mechanical conditioning of isolated chondrocytes in alginate it is necessary to determine the influence of compression on potential signalling events.

The aim of the present study was, therefore, to quantify cell and nucleus deformation in compressed alginate constructs. Due to the viscoelastic nature of the system and the possibility of active remodelling, the study examined both the initial deformation and any subsequent changes in morphology during prolonged static compression. The relationship between cell deformation and alginate concentration was also examined by measuring temporal changes in cell deformation in both 2% and 1.2% alginate constructs.

2. Materials and methods

2.1. Preparation of chondrocyte–alginate constructs

Articular chondrocytes were isolated from the metacarpal-phalangeal joint of 18 month old steers using a well characterised sequential enzymatic digestion procedure with pronase (700 units ml^{-1}, BDH, Poole, UK) and collagenase type XI (100 units ml^{-1}, Sigma, Poole, UK) [20]. The isolated cells were washed and resuspended in Dulbecco's minimal essential medium supplemented with 20% fetal calf serum (DMEM+20% FCS, Gibco, Paisley, UK). Other medium additives were streptomycin (5 mg ml^{-1}), L-glutamine (2 μM), HEPES (20 mM) and L-ascorbic acid (0.85 mM) (all supplied by Gibco).

GMB low viscosity alginate gel (Kelco) was prepared in Earle's balanced salt solution (EBSS, Gibco) at twice the required final concentration and sterilised by autoclaving. Equal volumes of cell suspension and alginate solution were mixed together to yield a final alginate concentration of 2% (w/v) with a cell density of 4×10^6 cells ml^{-1}. The cell–alginate suspension was poured into 10 mm diameter dialysing tubes (Spectrum Labs), which were immersed in 100 mM $CaCl_2$ in DMEM+20% FCS at 37°C for 90 min. The dialysing tubes were subsequently opened and the cell–alginate cut, using a series of parallel razor blades, into individual cores, 10 mm in diameter and 5 mm in height. The cores were secondarily cross-linked for 15 min at 37°C in DMEM+20% FCS supplemented with 100 mM $CaCl_2$. Cores were then maintained for approx. 20 h in DMEM+20% FCS within a humidified tissue culture incubator controlled at 37°C and 5% CO_2. Immediately prior to analysis of cell and nucleus morphology or mechanical testing, the alginate constructs were cut longitudinally into half cores.

2.2. Temporal changes in cell and nucleus morphology in compressed 2% alginate

Half core cell–alginate constructs (2% w/v) were incubated for 45 min at 37°C in a solution of calcein-AM (5 μM, Molecular Probes, USA) and Hoechst 33258 (5 μM, Sigma) prepared in DMEM+20% FCS. Individual constructs were mounted in a specially designed compression rig as described in previous studies [20,21]. The compression rig was placed upon the stage of an inverted microscope (TE200, Nikon, Kingston upon Thames, UK) associated with a confocal laser scanning microscope (Noran Oz, Thermo Microscopes, Bicester, UK). Confocal images of individual cells and associated nuclei in the central region of the construct, approx. 100 μm from the surface, were obtained using a $\times$40/0.95 NA objective lens (Nikon). For visualisation of viable cells labelled with calcein-AM, laser excitation was provided at a wavelength of 488 nm, with fluorescent light detected above a wavelength of 500 nm. For visualisation of cell nuclei labelled with Hoechst, an excitation wavelength of 364 nm was employed with emissions detection above 400 nm.

Individual cells and their nuclei were imaged in an unstrained construct by making a single confocal section image bisecting the centre of the cell and a second image bisecting the centre of the nucleus as previously described [20]. The position of the centre of the cell or nucleus was selected by adjusting the position of the focal plane during real time confocal imaging. A 20% uniaxial compressive strain was then applied to the construct at a strain rate of 5% s^{-1}, by means of a plunger driven by a computer controlled stepping linear actuator with a step size of 0.025 mm. Transmitted light microscopy was used to follow the selected cells during the application of compression to ensure that the same cells were imaged in both the unstrained and compressed state. The selected cells and their nuclei were imaged at two time points, approx. 5 min and 25 min after the start of compression. Approx. 5 cells and their nuclei were imaged within each construct. The procedure was repeated using a new construct on each occasion, to yield a total sample population of $n=30$.

The confocal image analysis software (Noran Intervision, Thermo Microscopes) was used to measure the cell and nucleus diameter parallel (X) and perpendicular (Y) to the axis of compression. Measurements were made to a precision of approx. 1 pixel, equivalent to 0.13 μm. The degree of deformation for both cell and nucleus was quantified in terms of the X and Y diameter strains, defined as the percentage change from the unstrained state (Appendix, Eqs. A1 and A2).

Previous studies using an identical loading regime demonstrated that isolated chondrocytes in compressed agarose constructs deformed from a spherical to an oblate ellipsoid such that for cell diameters $X<Y=Z$ [20,22]. Therefore, in the present study, the equation for the volume of an oblate ellipsoid was used to calculate the com-

pression induced percentage change in cell volume based on X and Y diameter measurements (Appendix, Eq. A4).

Statistical analysis was conducted using parametric Student's t-tests for either paired or non-paired data and with $P < 0.05$ indicating a statistically significant difference.

2.3. Influence of alginate concentration on cell deformation

To investigate the influence of alginate concentration on cell deformation, both 1.2% (w/v) and 2% (w/v) alginate half core constructs were prepared in an identical manner to that described above. Cells were labelled with calcein-AM and visualised using confocal laser scanning microscopy. Confocal section images were made bisecting the centre of individual cells ($n \approx 100$) in unstrained alginate constructs. Individual constructs were then compressed to 20% strain at a strain rate of 5% s^{-1} and a new sample of cells ($n \approx 30$) imaged over a 60 min period of static compression. For each cell the time of imaging was recorded relative to the start of compression as performed in previous studies [21]. The procedure was repeated using a new construct each time ($n = 3$) to yield a total sample size of approx. 100 cells for each alginate concentration. Cell X and Y diameters were measured and the diameter ratio, X/Y, calculated for each cell.

2.4. Influence of alginate concentration on mechanical properties

Cell free 1.2% (w/v) and 2% (w/v) alginate half core constructs were employed for mechanical characterisation. Constructs were mounted on a LRX materials testing machine (Lloyd Instrument, Farnham, UK) in a radially unconfined configuration between impermeable platens and hydrated in DMEM+20% FCS. A 20% uniaxial compressive strain was then applied at a strain rate of 5% s^{-1}. The applied strain was maintained for 60 min with load recorded at a sampling frequency of 18 Hz using a 10 N load cell. The procedure was repeated, using a new construct each time, to produce a total of six specimens for each alginate concentration. The cross-sectional area of each construct was measured from a projected image of a 1 mm thick transverse section cut from each construct and enlarged approx. $\times 30$ using an overhead projector. The applied load recorded by the load cell was dividing by the cross-sectional area of the construct to yield the applied stress.

3. Results

3.1. Temporal changes in cell and nucleus morphology in compressed 2% alginate

Individual cells and their nuclei in 2% alginate were imaged 5 ± 1 and 25 ± 3 (mean ± S.E.M.) min after the start of compression. Representative confocal images of a single cell and its nucleus in the unstrained state and at both time points in the compressed state are shown in Fig. 1. A 20% gross compression resulted in cell deformation from a spherical to an ellipsoid morphology. This cell deformation was characterised by a reduction in X diameter of $18.5 \pm 0.8\%$ (mean ± S.E.M.) and a corresponding increase in Y diameter of $16.9 \pm 1.6\%$, measured 5 min

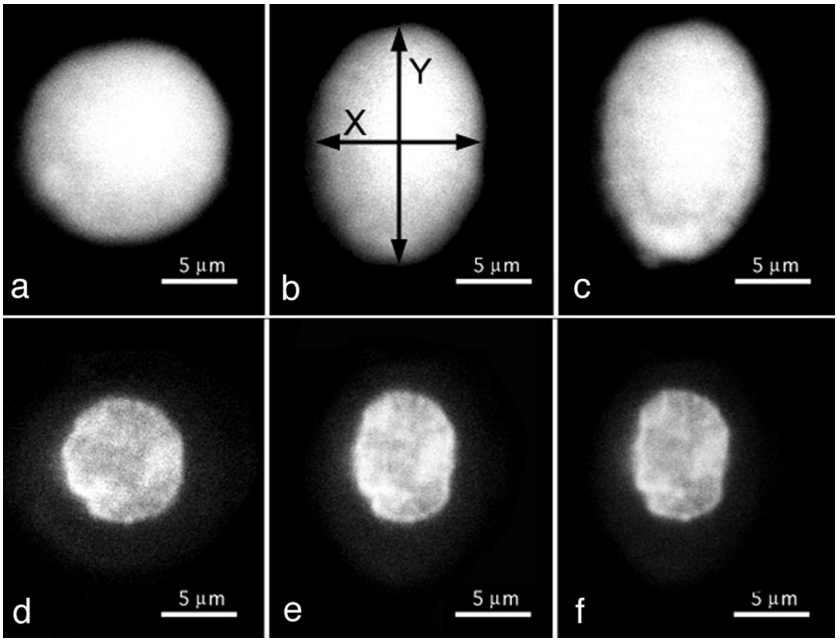

Fig. 1. Confocal images of a representative cell (a–c) and its nucleus (d–f) visualised in an unstrained 2% alginate construct (a,d) and after 5 min (b,e) and 25 min (c,f) of 20% static compression. Cells and nuclei were labeled with calcein-AM and Hoechst respectively. Scale bars indicate 5 μm. The cell X and Y diameters have been indicated parallel and perpendicular to the axis of compression.

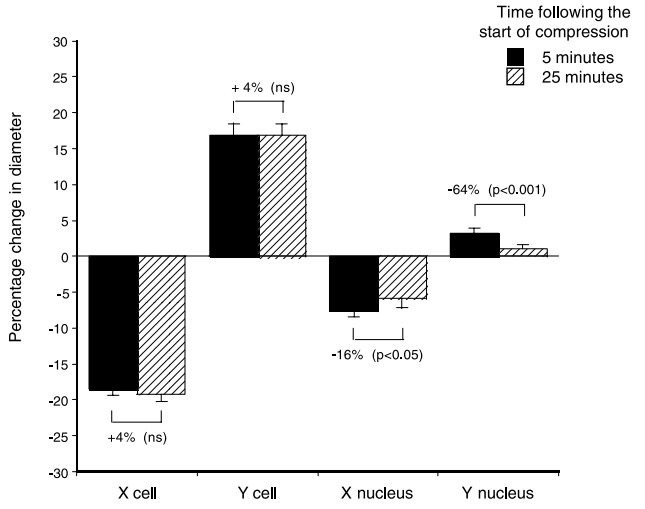

Fig. 2. Compression induced cell and nucleus X and Y diameter strains in 2% alginate measured 5 and 25 min after the application of 20% gross compression. Values represent sample means with error bars indicating S.E.M. for $n=20$ (cell deformation) and $n=30$ (nucleus deformation). The mean percentage changes between the two time points and the statistical significance are given based on the paired data.

after the start of compression (Fig. 2). Deformation occurred with an increase in cell volume of $12.0\pm3.4\%$ (mean $\pm$ S.E.M.), although this was not statistically significant ($P>0.05$). Cell deformation resulted in a change in nuclear morphology with a reduction in nucleus X diameter of $7.6\pm0.8\%$ (mean $\pm$ S.E.M.) and an associated increase in Y diameter of $3.2\pm0.7\%$ (Fig. 2). The nucleus X and Y diameter strains were substantially less than the corresponding values for cells, the differences being statistically significant ($P<0.001$).

Fig. 2 also indicates the deformation values for cell and nucleus, after 25 min of static compression. There were no statistically significant differences in the cell X and Y diameter strains between the two time points. However, there were statistically significant reductions in the magnitudes of nucleus deformation, with a 16% reduction in X diameter strain and a 60% reduction in Y diameter strain (Fig. 2).

3.2. Influence of alginate concentration on cell deformation

In the unstrained state, the isolated cells uniformly adopted a spherical morphology, as indicated by mean cell diameter ratios of 0.99 and 0.97 in 1.2% and 2% alginate, respectively. There was no statistically significant difference in the size of cells in 1.2% and 2% alginate, with unstrained diameters of 12.16 ± 1.19 μm (mean $\pm$ S.D.) and 12.13 ± 1.75 μm, respectively.

Fig. 3 indicates the temporal variation in cell diameter ratios (X/Y) over a 60 min period of 20% gross compression for samples of cells in both alginate concentrations. In both cases, compression resulted in an immediate cell deformation characterised by diameter ratios of approx. 0.70. In 2% alginate there was minimal subsequent change in the level of cell deformation over a 60 min period of compression, as reflected by the linear model ($r=0.32$, $P>0.05$). By contrast, in 1.2% alginate there was a marked increase in diameter ratio, indicating a recovery in cell deformation, returning towards a more spherical morphology. The rate of recovery was greatest immediately following compression but subsequently reduced (Fig. 3). The nature of this recovery in cell deformation in 1.2% alginate was modelled by a logarithmic relationship, which was statistically significant ($r=0.75$, $P<0.001$).

3.3. Influence of alginate concentration on mechanical properties

Both alginate constructs exhibited characteristic visco-

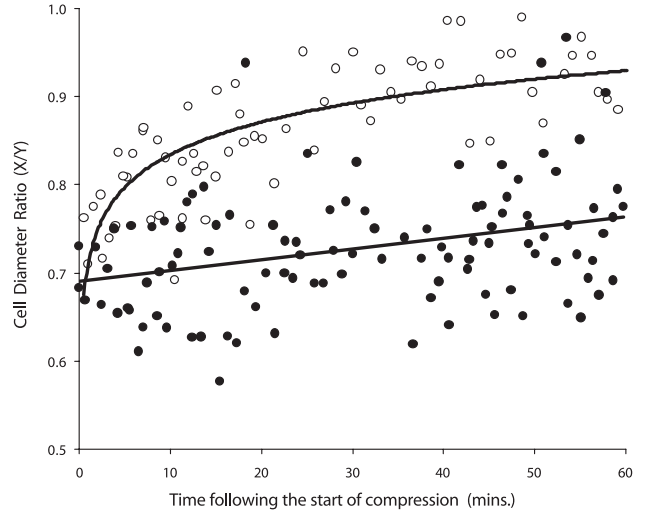

Fig. 3. Diameter ratios (X/Y) for isolated chondrocytes in 1.2% (○) and 2% (●) alginate constructs compressed to 20% static strain for a period of 60 min. Models of the form $X/Y=0.053\ln(t)+0.71$ ($r=0.75$, $P<0.001$) and $X/Y=0.0012(t)+0.69$, ($r=0.33$, $P>0.05$) have been fitted to the data for 1.2% and 2% alginate, respectively.

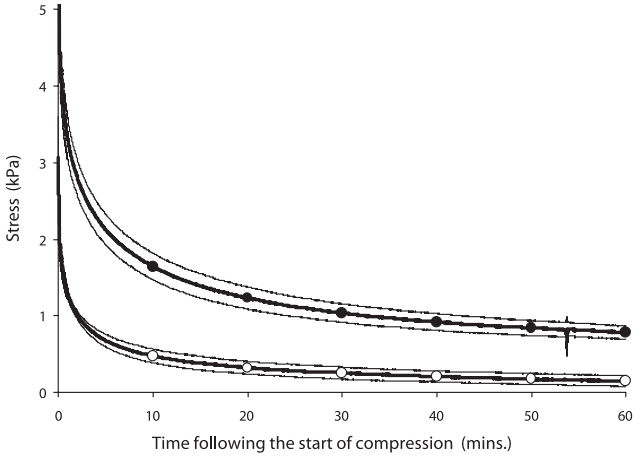

Fig. 4. Stress relaxation over a 60 min period of 20% static compression of 1.2% (○) and 2% (●) alginate constructs. Curves represent the mean values $\pm$ S.D. for $n=6$.

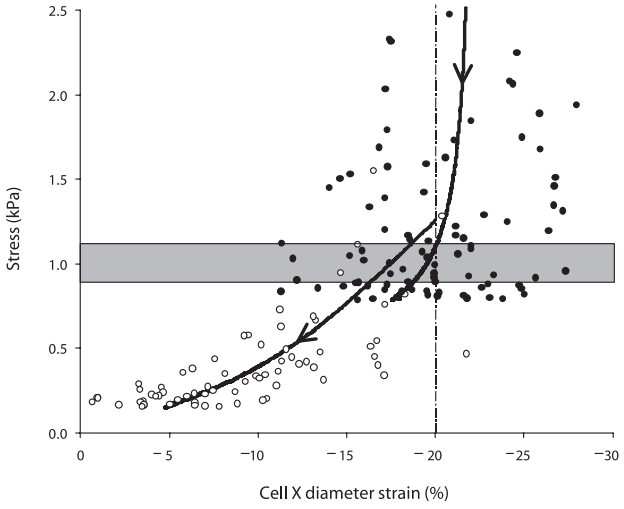

Fig. 5. Values of cell X diameter strain converted from cell diameter ratio measurements (Fig. 3) using Eq. A7 (Appendix) and plotted against the corresponding instantaneous stress values in compressed 1.2% (○) and 2% (●) alginate constructs (Fig. 4). Trend lines have been superimposed based on the curve fit models in Fig. 3, converted to X diameter strains, and plotted against the corresponding stress values for time, $t = 1$–60 min. The arrows indicate the temporal changes over a 60 min period of static 20% compression. The shaded area indicates a threshold value of approx. 1 kPa, such that above this threshold cell strain is approx. equal to applied strain and independent of applied stress.

elastic behaviour as shown by the representative stress relaxation graphs presented in Fig. 4. Following the application of the 20% compressive strain, the applied stress decreased rapidly at first and then more slowly. The relaxation moduli measured 60 min after the start of compression were 0.76 ± 0.34 kPa (mean ± S.D.) and 3.92 ± 0.4 kPa for 1.2% and 2% alginate, respectively.

4. Discussion

Previous studies have suggested that cell deformation may be a primary mechanotransduction mechanism for chondrocytes within intact articular cartilage and isolated in 3D scaffolds [10–12,23]. The downstream signalling pathways associated with cell deformation remain unclear, but may involve mechanosensitive membrane ion channels and associated changes in intracellular calcium [24–26], integrins [27], membrane perturbation and the inositol system [28], or deformation of intracellular organelles such as the cytoskeleton, rough endoplasmic reticulum and nucleus [8,29–31]. The direct effect of mechanical forces on nuclear function is poorly understood, although it has been suggested that nuclear deformation may influence nuclear transport and gene expression [10].

Alginate has been proposed as a scaffold component for tissue engineered cartilage repair due to its similarity to negatively charged proteoglycan and lack of toxicity [15,16]. In addition, isolated chondrocytes seeded in alginate gels have been shown to maintain a chondrocytic phenotype as demonstrated by the synthesis of cartilaginous matrix [32]. However, the mechanotransduction signalling pathways within cell seeded alginate gels may differ from those within intact cartilage as well as those within non-charged hydrogel scaffolds such as agarose. Cell and nucleus morphologies in unstrained and compressed alginate constructs were examined using confocal microscopy techniques similar to those used in previous studies [20,33]. Compression of 2% alginate constructs resulted in cell deformation characterised by a reduction in X diameter, approximately equal to the applied strain, and an increase in Y diameter (Figs. 1 and 2). There was no statistically significant change in cell volume, similar to that reported in agarose [20], but in contrast to the reduction in cell volume in compressed cartilage explants [6–8]. The behaviour in cartilage may be due to a reduction in osmotic pressure caused by compression of the negatively charged extracellular matrix [11]. Although alginate gels are also negatively charged, they exhibit a limited charged density compared to that of proteoglycan-rich cartilage matrix. Hence any compression induced osmotic change in 2% alginate may be insufficient to elicit a reduction in cell volume. Alternatively, the reduction in cell volume in intact cartilage may be due to the matrix preventing lateral expansion during compression, such that the resulting intracellular hydrostatic pressure causes fluid transport across the cell membrane. This hypothesis is supported by a previous study in which a 20% reduction in cell X diameter in compressed cartilage was associated with an increase in Y diameter of less than 4% [6], compared to the increase of 16% measured in alginate in the present study.

Cell deformation was associated with deformation of the nucleus, possibly mediated through cytoskeletal components, such as the vimentin intermediate filament network, which form a mechanical link between the cell membrane and the nucleus [30,31,34]. The nucleus diameter strains were significantly less than those experienced by the cells, as reported for chondrocytes compressed in agarose constructs [20] and in cartilage explants [7]. These findings suggest that the nucleus is stiffer than the surrounding cytoplasm, in agreement with a previous pipette aspiration study, which estimated a modulus value for the nucleus which was approx. 10 times greater than that of the chondrocyte [35].

By imaging the same individual chondrocytes and their nuclei at two time points, approx. 5 and 25 min after the start of compression, it was possible to examine temporal changes in cell and nucleus deformation. Despite the constant cell deformation in compressed 2% alginate, there was a significant temporal recovery in nucleus deformation in both the X and Y directions (Fig. 2). This recovery in nuclear morphology may involve nuclear reorganisation and a reduction in nuclear volume. This behaviour may be associated with cytoskeletal reorganisation, which has been shown to occur following deformation of articular chondrocytes compressed in agarose constructs [36] and

in cartilage explants [37,38]. However, it remains unclear whether the changes in nucleus morphology are due to passive viscoelastic behaviour or active remodelling of the nucleus and/or the cytoplasmic components.

Previous studies have employed various concentrations of alginate gel in which to examine the behaviour of chondrocytes and the influence of mechanical loading. Two of the most common alginate concentrations, namely 1.2% and 2%, were investigated in the present study. Mechanical characterisation was conducted in unconfined uniaxial compression to simulate the loading regime employed for analysis of cell deformation. Both concentrations of alginate exhibited time-dependent stress relaxation behaviour, characteristic of a viscoelastic material (Fig. 4). Unlike the stress relaxation behaviour of agarose gels in which the stress reaches an equilibrium after 5–15 min [39], the stress within both alginate gel concentrations continued to relax over the 60 min period. Increasing the alginate concentration increased the moduli of the resulting constructs as previously reported [40].

The concentration of alginate did not influence either the shape or the diameter of unstrained chondrocytes. The regular spherical morphology in the unstrained state enabled cell deformation during compression to be quantified in terms of a diameter ratio, as adopted in previous studies [21,33,41]. Cell X and Y diameter strains were calculated from diameter ratios using the equations derived in the appendix (Appendix, Eqs. A7 and A8).

Compression of both 2% and 1.2% alginate constructs yielded levels of cell deformation which were initially of a similar magnitude, with diameter ratios of approx. 0.70 (Fig. 3), equivalent to an X diameter strain of -20%. However, in contrast to the behaviour in 2% alginate where cell deformation remained approximately constant, the magnitude of cell deformation in 1.2% alginate subsequently reduced in association with the stress relaxation exhibited by the alginate (Fig. 4). Thus after 60 min of static compression the cells were almost spherical, with diameter ratios of approx. 0.92, equivalent to an X diameter strain of -5% (Fig. 3). Similar recovery in cell deformation has previously been reported for chondrocytes compressed in 1% [42] and 2% agarose gel [41]. In the latter study, this behaviour was attributed to an active cellular response to applied compression. However, this explanation is unlikely to be true since there is minimal relaxation of cell deformation when cells are compressed in stiffer gels such as 2% alginate (Fig. 3) or 3% and 4% agarose [20–22,26,33,39,42]. Therefore, the reported relaxation in cell deformation within 1.2% alginate constructs appears to be a direct result of the viscoelastic behaviour of the lower stiffness alginate substrate.

To examine this hypothesis, the cell X diameter strains, calculated from diameter ratios in 1.2% and 2% alginate (Fig. 3), were plotted against the instantaneous total stress in the corresponding alginate using the mean value of six replicates (Fig. 4). This yielded the stress versus cell strain relationship shown in Fig. 5. This figure presents the superimposed trend lines based on the curve fit models in Fig. 3, converted to X diameter strains, for time, $t = 1$–60 min. The figure indicates the presence of a threshold stress value at approx. 1 kPa (Fig. 5). Above this stress threshold, the cell X diameter strain is equal to the applied compressive strain of 20%. However, below the threshold the stress generated in the compressed construct is insufficient to maintain the cell X diameter strain at the 20% level. Hence, in compressed 1.2% alginate constructs, the magnitude of cell deformation reduces as the stress in the alginate relaxes below the 1 kPa threshold (Figs. 3–5). The precise value of the threshold is dependent on the applied strain, but the general behaviour is fundamental to all homogenous scaffolds providing the cell volume fraction is relatively small.

Within biphasic materials, compression induces both multidirectional fluid stress and unidirectional solid stress. Cell strain is a function of solid stress and independent of fluid stress. We propose that low concentration hydrogels, such as alginate, behave primarily like viscoelastic solids with a minimal fluid stress component. Thus the data below the threshold in Fig. 5 represent the stress–strain properties of the cell with a toe-in region at low strains followed by a more linear region. This characteristic nonlinear behaviour may be associated with so-called 'strain stiffening' of the cytoskeleton [43,44] or recruitment of nuclear deformation. A linear model was fitted to the data corresponding to X diameter strains between 0% and -15%. The gradient of this linear model represents an estimate of the Young's modulus of the cell with a value of 3.2 ± 0.5 kPa. This value is close to the modulus of 4.0 kPa calculated by Freeman et al. using finite element analysis of cell deformation in compressed agarose [41]. By contrast, the Young's modulus of isolated chondrocytes has previously been estimated at approx. 0.5 kPa using pipette aspiration techniques [45,46]. However, direct mechanical perturbation techniques such as pipette aspiration, atomic force microscopy or cell poking provide localised properties, which may be primarily influenced by structures closely associated with the cell membrane such as the cortical actin cytoskeleton, rather than gross mechanical properties. Furthermore, the gross cell stiffness values obtained using these methods are heavily dependent on the theoretical models used for data interpretation. By contrast, the method developed in the present study provides a new and important experimental approach for estimating gross cellular mechanical properties during physiological loading in 3D scaffolds. The results suggest that the gross modulus of isolated chondrocytes is greater than previous estimates.

In conclusion, this study provides important morphological and mechanical data, which will assist the understanding of how isolated chondrocytes respond to compressive loading within a range of different tissue engineered cartilage repair systems.

Acknowledgements

This study was conducted during a research visit to the IRC in Biomedical Materials by J.v.d.B.B. supported on an Erasmus Student Scholarship. The Engineering and Physical Sciences Research Council provides core funding for the IRC in Biomedical Materials and supports M.M.K. as an Advanced Research Fellow.

Appendix. Calculation of cell diameter strain from diameter ratio *X*/*Y*

The suffixes 's' and 'u' denote the strained and unstrained states respectively whilst X and Y represent the cell diameters measured parallel and perpendicular to the axis of compression.Cell X diameter strains,

$$\varepsilon_X = \frac{X_s - X_u}{X_u} \times 100\% \quad \text{(A1)}$$

$$\varepsilon_Y = \frac{Y_s - Y_u}{Y_u} \times 100\% \quad \text{(A2)}$$

Cell volume – unstrained ($X = Y = Z$)

$$V_u = \frac{\pi X_u^3}{6} \quad \text{(A3)}$$

Cell volume – compressed ($X < Y = Z$)

$$V_s = \frac{\pi X_s Y_s^2}{6} \quad \text{(A4)}$$

In the present study measurements of the same individual cells in both the unstrained and compressed state indicated that cell deformation occurred with no statistically significant change in cell volume. Thus,

$$V_u = V_s \quad \text{(A5)}$$

By substituting Eqs. A3 and A4 into Eq. A5 yields:

$$Y_u = X_u = (X_s Y_s^2)^{1/3} \quad \text{(A6)}$$

Substituting Eq. A6 into Eqs. A1 and A2 yields the following expressions, where X_s/Y_s represents the diameter ratio of the compressed cell:

$$\varepsilon_X = \left(\left(\frac{X_s}{Y_s} \right)^{2/3} - 1 \right) \times 100\% \quad \text{(A7)}$$

$$\varepsilon_Y = \left(\left(\frac{X_s}{Y_s} \right)^{3/2} - 1 \right) \times 100\% \quad \text{(A8)}$$

References

[1] G. Vunjak-Novakovic, B. Obradovic, I. Martin, P.M. Bursac, R. Langer, L.E. Freed, Biotechnol. Prog. 14 (1998) 193–202.
[2] R. Langer, J.P. Vacanti, Science 260 (1993) 920–926.
[3] K.T. Paige, L.G. Cima, M.J. Yaremchuk, J.P. Vacanti, C.A. Vacanti, Plast. Reconstr. Surg. 96 (1995) 1390–1398.
[4] G. Vunjak-Novakovic, B. Obradovic, S. Treppo, A.J. Grodzinsky, R. Langer, L.E. Freed, J. Orthop. Res. 17 (1999) 130–138.
[5] R.L. Mauck, M.A. Soltz, C.C.B. Wang, D.D. Wong, P.-H.G. Chao, C.T. Hung, G.A. Ateshian, J. Biomech. Eng. 122 (2000) 252–260.
[6] F. Guilak, A. Ratcliffe, V.C. Mow, J. Orthop. Res. 13 (1995) 410–421.
[7] F. Guilak, J. Biomech. 28 (1995) 1529–1541.
[8] M.D. Buschmann, E.B. Hunziker, Y.J. Kim, A.J. Grodzinsky, J. Cell Sci. 109 (1996) 499–508.
[9] C.A. Heath, S.R. Magari, Biotechnol. Bioeng. 50 (1996) 430–437.
[10] F. Guilak, R. Sah, L.A. Setton, in: V.C. Mow, W.C. Hayes (Eds.), Basic Orthopaedic Biomechanics, Lippincott-Raven, 1997, pp. 179–207.
[11] J.P.G. Urban, Br. J. Rheumatol. 33 (1994) 901–908.
[12] D.A. Lee, D.L. Bader, J. Orthop. Res. 15 (1997) 181–188.
[13] M.D. Buschmann, Y.A. Gluzband, A.J. Grodzinsky, E.B. Hunziker, J. Cell Sci. 108 (1995) 1497–1508.
[14] P.M. Ragan, V.I. Chin, H.K. Hung, K. Masuda, E.J.M.A. Thonar, E.C. Arner, A.J. Grodzinksy, J.D. Sandy, Arch. Biochem. Biophys. 383 (2000) 256–264.
[15] G. Skjak-Braek, Biochem. Soc. Trans. 20 (1992) 27–33.
[16] K.T. Paige, L.G. Cima, M.J. Yaremchuk, B.L. Schloo, J.P. Vacanti, C.A. Vacanti, Plast. Reconstr. Surg. 97 (1996) 168–178.
[17] C. Perka, R.S. Spitzer, K. Lindenhayn, M. Sittinger, O. Schultz, J. Biomed. Mater. Res. 49 (2000) 305–311.
[18] S.C. Chang, J.A. Rowley, G. Tobias, N.G. Genes, A.K. Roy, D.J. Mooney, C.A. Vacanti, L.J. Bonassar, J. Biomed. Mater. Res. 55 (2000) 503–511.
[19] E. Fragonas, M. Valente, M. Pozzi-Mucelli, R. Tofffanin, R. Rizzo, F. Silvestri, F. Vittur, Biomaterials 21 (2000) 795–801.
[20] D.A. Lee, M.M. Knight, J.F. Bolton, B.D. Idowu, M.V. Kayser, D.L. Bader, J. Biomech. 33 (2000) 81–95.
[21] M.M. Knight, S.A. Ghori, D.A. Lee, D.L. Bader, J. Med. Eng. Phys. 20 (1998) 684–688.
[22] M.M. Knight, PhD Thesis, University of London, 1997.
[23] D.E. Ingber, in: V.C. Mow, F. Guilak, R. Tran-Son-Tay, R.M. Hochmuth (Eds.), Cellular Mechanics and Mechanotransduction, Springer-Verlag, 1994, pp. 329–342.
[24] F. Sachs, Mol. Cell. Biochem. 104 (1991) 57–60.
[25] F. Guilak, R.A. Zell, G.R. Erickson, D.A. Grande, C.T. Rubin, K.J. McLeod, H.J. Donahue, J. Orthop. Res. 17 (1999) 421–429.
[26] S.R. Roberts, M.M. Knight, D.A. Lee, D.L. Bader, J. Appl. Physiol. 90 (2001) 1385–1391.
[27] S.J. Millward-Sadler, M.O. Wright, H.S. Lee, K. Nishida, H. Caldwell, G. Nuki, D.M. Salter, J. Cell Biol. 145 (1999) 183–189.
[28] M. Berridge, R. Irvine, Nature 341 (1989) 197–205.
[29] N. Wang, J.P. Butler, D.E. Ingber, Science 260 (1993) 1124–1127.
[30] D. Ingber, Curr. Opin. Cell Biol. 3 (1991) 841–848.
[31] P.A. Janmey, Physiol. Rev. 78 (1998) 763–781.
[32] H.J. Hauselmann, R.J. Fernandes, S.S. Mok, T.M. Schmid, J.A. Block, M.B. Aydelotte, K.E. Kuettner, J.M.A. Thonar, J. Cell Sci. 107 (1994) 17–27.
[33] M.M. Knight, D.A. Lee, D.L. Bader, Biochim. Biophys. Acta 1405 (1998) 67–77.
[34] A.J. Maniotis, C.S. Chen, D.E. Ingber, Proc. Natl. Acad. Sci. USA 94 (1997) 849–854.
[35] F. Guilak, J.R. Tedrow, R. Burgkart, Biochem. Biophys. Res. Commun. 269 (2000) 781–786.
[36] D.A. Lee, M.M. Knight, B. Idowu, D.L. Bader, Trans. Orthop. Res. (2001) 263–263.
[37] L.A. Durrant, C.W. Archer, M. Benjamin, J.R. Ralphs, J. Anat. 194 (1999) 343–353.
[38] E. Langelier, R. Suetterlin, U. Aebi, M.D. Buschmann, Trans. Orthop. Res. Soc. (1999) 631.

[39] M.M. Knight, D.A. Lee, D.L. Bader, J. Cell. Eng. 1 (1996) 97–102.
[40] M.A. LeRoux, F. Guilak, L.A. Setton, J. Biomed. Mater. Res. 47 (1999) 46–48.
[41] P.M. Freeman, R.N. Natarajan, J.H. Kimura, T.P. Andriacchi, J. Orthop. Res. 12 (1994) 311–320.
[42] M.M. Knight, D.A. Lee, D.L. Bader, Trans. Eur. Soc. Biomech. (2000) 323.
[43] K.Yu. Volokh, O. Vilnay, M. Belsky, J. Biomech. 33 (2000) 1543–1549.
[44] J. Xu, Y. Tseng, D. Wirtz, J. Biol. Chem. 275 (2000) 35886–35892.
[45] F. Guilak, W.R. Jones, P. Ting-Beall, G.M. Lee, Osteoarthritis Cartilage 7 (1999) 59–70.
[46] W.R. Jones, H.P. Ting-Beall, G.M. Lee, S.S. Kelley, R.M. Hochmuth, F. Guilak, J. Biomech. 32 (1999) 119–127.